Visibility diagrams and experimental stripe structures in the quantum Hall effect

2000 J. Phys. A: Math. Gen. 33 8649

(http://iopscience.iop.org/0305-4470/33/48/305)

J. Phys. A: Math. Gen. **33** (2000) 8649–8662. Printed in the UK PII: S0305-4470(00)12222-X

Visibility diagrams and experimental stripe structures in the quantum Hall effect

Yvon Georgelin†, Thierry Masson‡ and Jean-Christophe Wallet†

† Groupe de Physique Théorique, Institut de Physique Nucléaire, F-91406 Orsay Cedex, France
‡ Laboratoire de Physique Théorique (UMR 8627), Université de Paris-Sud, Bâtiment 211, F-91405 Orsay Cedex, France

Received 28 February 2000, in final form 14 July 2000

Abstract. We analyse various properties of the visibility diagrams that can be used in the context of modular symmetries and confront them with some recent experimental developments in the quantum Hall effect. We show that a suitable physical interpretation of the visibility diagrams, which permits one to describe successfully the observed architecture of the quantum Hall states, gives rise naturally to a stripe structure reproducing some of the experimental features that have been observed in the study of the quantum fluctuations of Hall conductance. Furthermore, we show new properties of the visibility diagrams stemming from the structure of subgroups of the full modular group.

1. Introduction

The quantum Hall effect (QHE) is a remarkable phenomenon occurring in a two-dimensional electron gas in a strong magnetic field at low temperature [1]. Since the discovery of the quantized integer [2] and fractional [3] Hall conductivity, the QHE has been an intensive area of theoretical and experimental investigation. The pioneering theoretical contributions [4] analysing the basic features of the hierarchy of the Hall plateaux have triggered numerous works aiming to provide a better understanding of the underlying properties governing the complicated phase diagram associated with the quantum Hall regime, together with the precise nature of the various observed transitions between plateaux and/or focusing on the characterization of a suitable theory.

It has been realized for some time that modular symmetries may well be of interest to understand more deeply some salient features of the QHE. For instance, it has been suggested [5–7] that some properties of the phase diagram may be explained in terms of modular group transformations. At the present time, a fully satisfactory microscopic or effective theory for the QHE, from which the relevant modular symmetry (if any) would arise, is still lacking. This has motivated further studies aimed at the derivation of general constraints on the phase diagram coming from the full modular group or some of its subgroups [6, 7].

Some time ago, we showed that a special subgroup of the full modular group, namely the group $\Gamma(2)$, can be used to derive a model for a classification of integer, as well as fractional, Hall states [9, 10]. We further showed that the constraints stemming from $\Gamma(2)$ on physically admissible β functions [11] give rise to a global phase diagram as well as crossover in the various observed transitions, which are in good agreement with the present experimental observations. Here, it is worth recalling that the classification based on the $\Gamma(2)$ symmetry [9, 10], which

0305-4470/00/488649+14$30.00

refines the Jain and Haldane ones, reproduces successfully the observed hierarchical structures of the Hall states. This construction can be somehow viewed as a modification of the law of the corresponding states proposed in [12], whose underlying symmetry group is larger than $\Gamma(2)$. This difference will be commented upon in the next section. The construction based on $\Gamma(2)$ involves two important building blocks (in addition to the action of the group $\Gamma(2)$ itself) called the visibility diagrams. Basically, these diagrams, inherited from theoretical studies in arithmetic and rigidly linked to the structure of $\Gamma(2)$, have been shown to encode a great amount of information on the experimentally observed global organization of the quantum Hall states.

Recently, some new experiments on mesoscopic conductance in the quantum Hall regime in silicon MOSFETs have been performed [13]. The essential experimental result is that the extrema of the conductance fluctuations in the quantum Hall regime spread on linear trajectories in the gate voltage V_g–magnetic field B plane, parallel to lines of constant filling factor $\nu = p$ (with $p = 0, 1, 2, \ldots$). In [13], the following relation:

$$\frac{C}{e}\frac{\partial V_g}{\partial B} = n\frac{e}{h} \qquad n \text{ integer} \tag{1.1}$$

in which $\frac{C}{e} = \frac{\partial \rho}{\partial V_g}$ is assumed to hold (ρ denotes the electron density and the constant $\frac{C}{e} = 8.6 \times 10^{11}$ cm^{-2} V^{-1} in [13]) has been found to be verified to within a few percent accuracy. Furthermore, a stripe structure in the V_g–B plane has been clearly observed in this experiment.

For the sake of clarity, we now summarize the principal result of this paper: the main (mathematical) features of one type of visibility diagram (hereafter called the odd visibility diagram) admit naturally a consistent physical interpretation, based principally on the very definition of the filling factor ν (recall that $\nu = \frac{N_c}{N_\Phi}$, where N_c and $N_\Phi = BS\frac{h}{e^2}$ (S is the device area) denote, respectively, the number of charge carriers and number of unit flux), combined with a physical interpretation of the generators of $\Gamma(2)$. This interpretation permits one to map the odd visibility diagram to the V_g–B plane so that:

(i) The stripe structure appearing in the odd diagram (in which each stripe is, by construction, rigidly linked to a Hall plateau) reproduces nicely the experimentally observed stripe structure reported in [13].

(ii) A consistent interpretation of (1.1) can be obtained within the proposed framework, thanks in particular to the fact that the lines passing through the origin of the odd visibility diagram are lines of constant filling factor.

This paper is organized as follows. In section 2.1, we collect useful properties of the group $\Gamma(2)$ and recall briefly the construction of the even visibility diagram, which basically permits one to visualize the architecture of the quantum Hall states obtained from $\Gamma(2)$ which fits well with the present experimental situation [10]. In section 2.2, we describe the construction of the odd visibility diagram which is a central element in this paper. Section 2.3 is devoted to the physical interpretation of the odd visibility diagram which makes it possible to map this to the V_g–B plane and to reproduce most of the experimental features obtained in [13]. Some new properties of the visibility diagrams stemming from the structure of subgroups of the modular group have been collected separately and are presented for the sake of completeness in section 3. Finally, we summarize the results and draw conclusions.

2. Visibility diagrams and stripe structures

2.1. Group $\Gamma(2)$*, classification of Hall states and even visibility diagram*

The possible importance of the role played by modular symmetries in the QHE has been considered for some time. Some of the related work has emphasized that (most of) the (up to now) experimentally observed features of QHE seem to be recovered from the action of a suitable subgroup of the modular group on the complex conductivity plane. This latter is denoted hereafter by $\bar{\mathcal{P}} \equiv \mathcal{P} \cup Q$ where $\mathcal{P}$ is the (open) upper half complex plane and Q is the set of rational numbers. The complex coordinate on $\bar{\mathcal{P}}$ is defined by $z = (\sigma_{xy} + i\sigma_{xx})$†, the complex conductivity, where σ_{xy} (resp. σ_{xx}) denotes the Hall (resp. longitudinal) conductivity.

Let us now recall the essential features of $\Gamma(2)$ that will be needed in the following analysis. The group $\Gamma(2)$ is the set of transformations G acting on $\bar{\mathcal{P}}$ which can be written as

$$G(z) = \frac{(2s+1)z + 2n}{2rz + (2k+1)} \qquad k, n, r, s \in Z \tag{2.1}$$

where

$$(2s+1)(2k+1) - 4rn = 1 \tag{2.2}$$

is the unimodularity condition. The two generators of $\Gamma(2)$ are defined by

$$T^2(z) = z + 2 \tag{2.3a}$$

$$\Sigma(z) = \frac{z}{2z+1}. \tag{2.3b}$$

Before proceeding further, one comment is in order. The group $\Gamma(2)$ is a subgroup of the symmetry group underlying the law of the corresponding states proposed in [12]. This latter group is known in the mathematical literature as $\Gamma_0(2)$ and is generated by $\Sigma(z)$ (2.3*b*), the flux attachment operator, and $T(z) = z + 1$, the Landau level addition operator. The physical assumption behind the Landau level addition symmetry is that the physics at any (partially filled) Landau level is independent of the number of completely filled lower Landau levels. Basically, this assumption, as pointed out and discussed in [8], seems to be reasonable for well separated Landau levels but may well become questionable whenever the Landau levels are organized into well separated pairs and lie close to each other within each pair, for instance due to spin splitting effects [8]. Then, the physics of the upper level of a given pair may well be influenced by the electrons located in the lower level of the pair, while it seems still plausible to assume that the physics of any pair is independent of how many pairs below are filled. Then, a possible way to take this into account is to replace the Landau level addition operator $T(z)$ by $T^2(z)$ given in (2.3*a*). The physical differences between $\Gamma(2)$ and $\Gamma_0(2)$ for their possible relevance to the QHE have been explored and discussed in [6–11] and the motivations for choosing $\Gamma(2)$ instead of any other possible subgroup of the modular group has already been presented in [11]. From these previous analyses, it appears that $\Gamma(2)$ is an appealing candidate for a possible symmetry group relevant to the QHE.

Now the construction of a model for the classification of the quantum Hall states based on $\Gamma(2)$ can be obtained, as already explained in [10], by restricting $\Gamma(2)$ to act only on the real part of the complex conductivity z, which is identified with the filling factor ν (parametrized as $\nu = p/q$). Then, as we have shown in [9], for a given (fixed) even denominator metallic state $\lambda = \frac{2s+1}{2r}$, the hierarchy of the (liquid) odd denominator states surrounding this metallic state is obtained from the images $G^{\lambda}_{n,k}(0)$ and $G^{\lambda}_{n,k}(1)$ of 0 and 1 by the family of transformations $G^{\lambda}_{n,k} \in \Gamma(2)$, where $\lambda = \frac{2s+1}{2r}$ holds and n, k are constrained by the unimodularity condition (2.2).

† Here we have set $e^2 = h = 1$; these quantities will be reinstated when necessary in the course of the analysis.

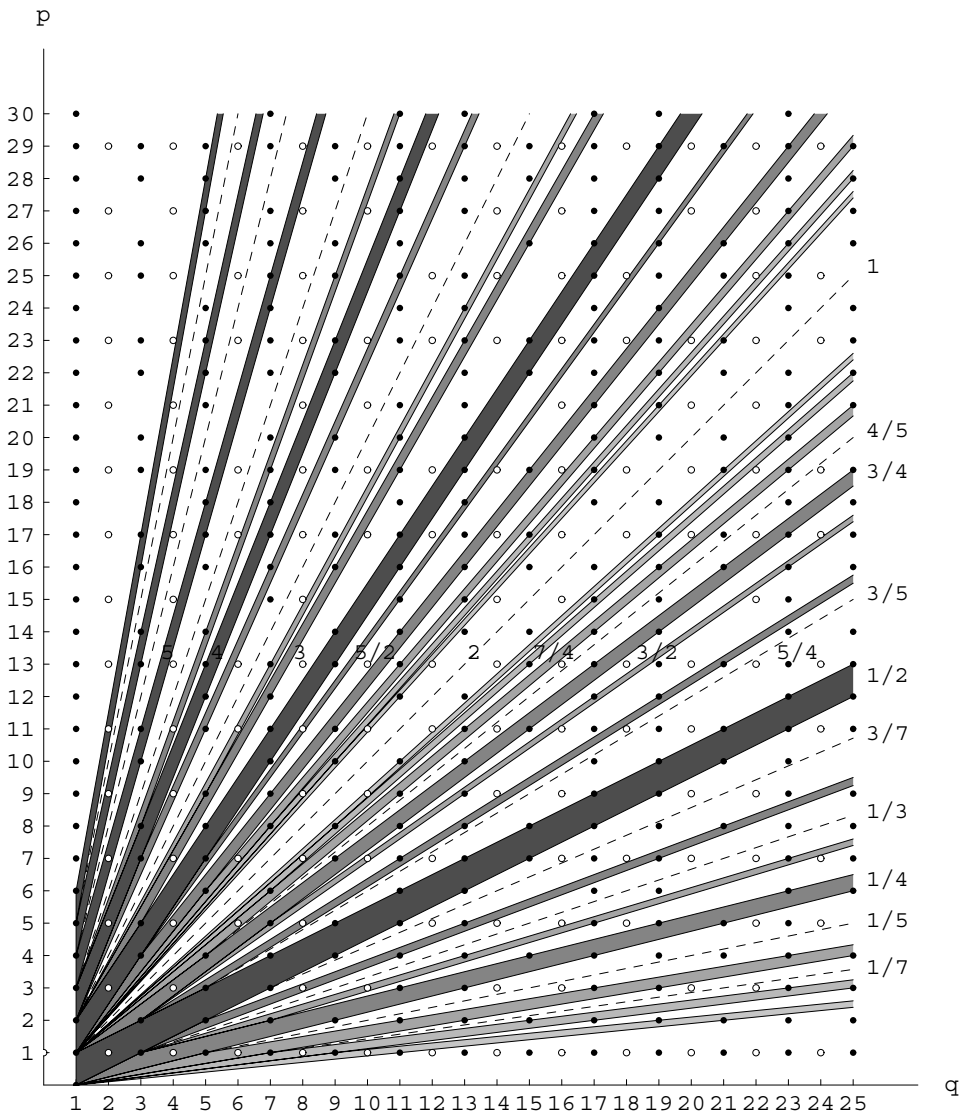

Figure 1. Even visibility diagram. The stripe indexed by 1/2 can be used to reproduce the Jain hierarchy. Open dots represent fractions p/q with q even, full dots represent fractions with q odd.

The action of $\Gamma(2)$ on the filling factor $\nu = p/q$ can be visualized with the help of graphical representations called visibility diagrams, whose construction is now summarized (for a detailed construction see [10]). Consider a two-dimensional square lattice whose vertices are indexed by a couple of positive (or zero) *relatively prime* integers (q, p). Since $\Gamma(2)$ preserves the parity of the denominator of any rational fraction, there are actually two ways to organize the vertices pertaining to this lattice, depending on whether the denominator is even or odd.

Consider first the case where it is even and choose therefore a given $\lambda = \frac{2s+1}{2r}$ as a starting vertex. Then, it is not difficult to realize that $G^{\lambda}_{n,k}(0)$ and $G^{\lambda}_{n,k}(1)$, which, in the present framework, label the Hall plateaux surrounding the even denominator (metallic) Hall

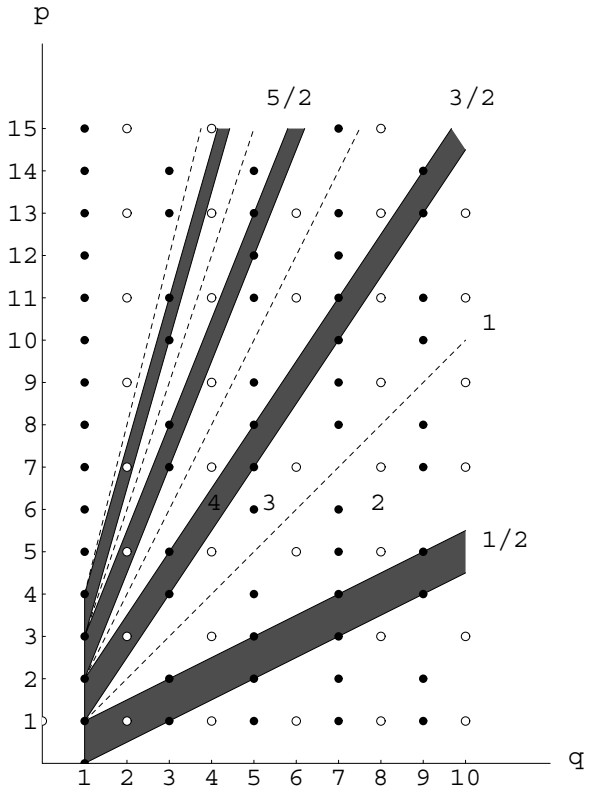

Figure 2. Selected stripes indexed by $\frac{2s+1}{2}$, s integer. Open dots represent fractions p/q with q even, full dots represent fractions with q odd. A comparison with figure 3 of [16] suggests to identify the vertical (half) stripe indexed by $q = 0$ and $p = 1$ with the insulator.

state corresponding to λ, are all located on two parallel straight lines forming an unbounded left-ended stripe surrounding the vertex λ. Finally, the application of a similar process to all even denominator fractions gives rise to a collection of non-overlapping stripes as depicted in figure 1, each stripe corresponding therefore to a vertex with even denominator. This visibility diagram, hereafter called the even diagram, involves naturally the Jain hierarchy, which corresponds to the stripe associated with $\lambda = 1/2$ as can be easily realized by computing the successive values for $G^{1/2}_{n,k}(0)$ and $G^{1/2}_{n,k}(1)$ using (2.1) and (2.2). It is worth recalling some experimental results performed in [14–16] on metal–insulator transitions. It appears that the corresponding phase diagrams (see, e.g. figure 2 of [14] and figure 2 of [15]; see also a recent result reported in [16]) exhibit a stripe structure which bears some similarity with the stripe structure occurring in the even diagram when, anticipating what will be done soon, the (q, p) plane is identified with the magnetic field-charge carrier density plane†. This can be easily illustrated by selecting from figure 1 the relevant stripes which correspond here to $\lambda = (2s+1)/2$, as shown in figure 2, to be compared with figure 3 of [16]. We mention, by the way, that a numerical determination of the phase diagram for the integer QHE (charge carrier density ($\sim V_g$) versus magnetic field) has been performed recently in [17]. The corresponding results seem to be (qualitatively) consistent with the experimental results obtained in [16].

† At least for not too small a charge carrier density.

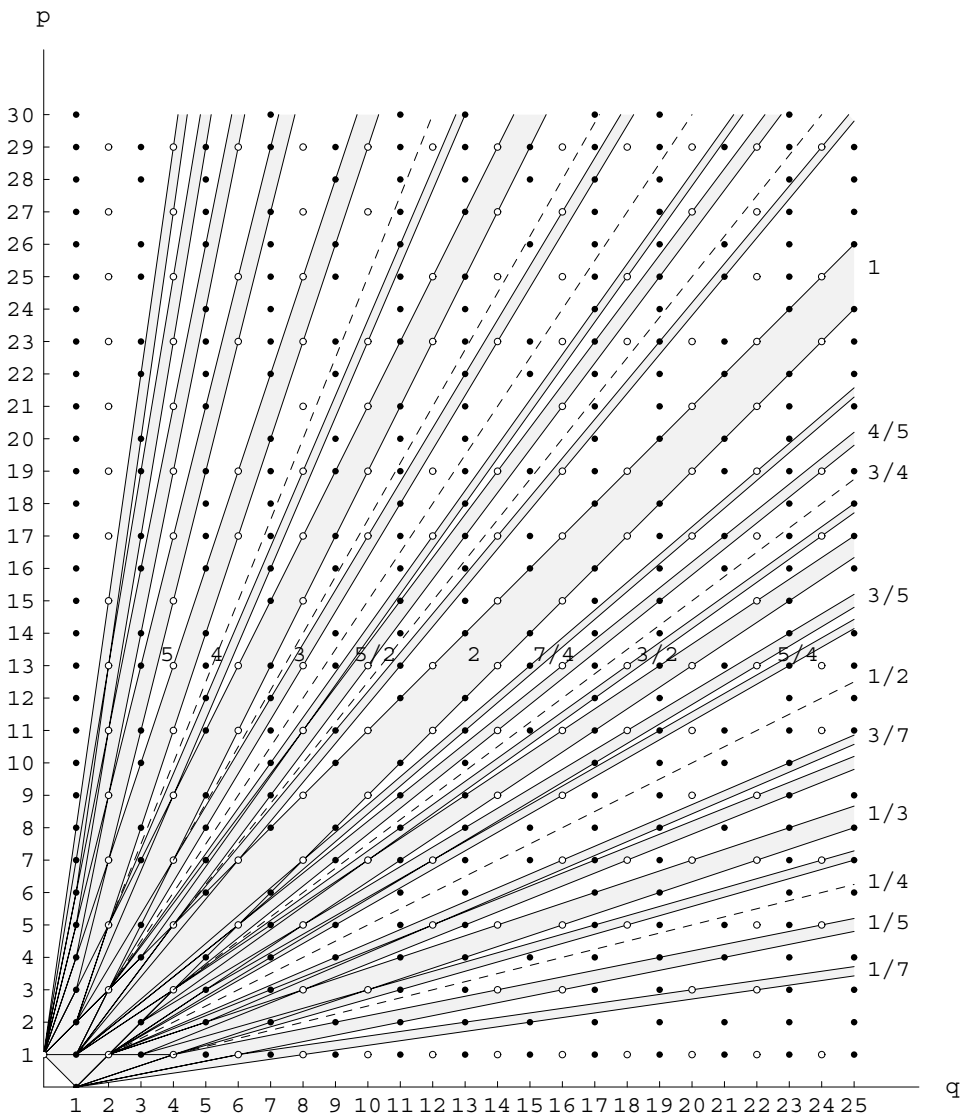

Figure 3. Odd visibility diagram. Open dots represent fractions p/q with q even, full dots represent fractions wtih q odd. In [10], a numerical simulation based on information encoded in this diagram was performed for the p_{xy} versus B plot.

Notice that, provided the above interpretation of the (q, p) plane is actually correct, the vertical leftmost half stripe (indexed by '1/0') that is involved in the even diagram might be associated with the insulator.

2.2. The odd visibility diagram

The second diagram that can be constructed, hereafter called the odd diagram, can be readily obtained by using a well known theorem in arithmetic which states that, for any relatively

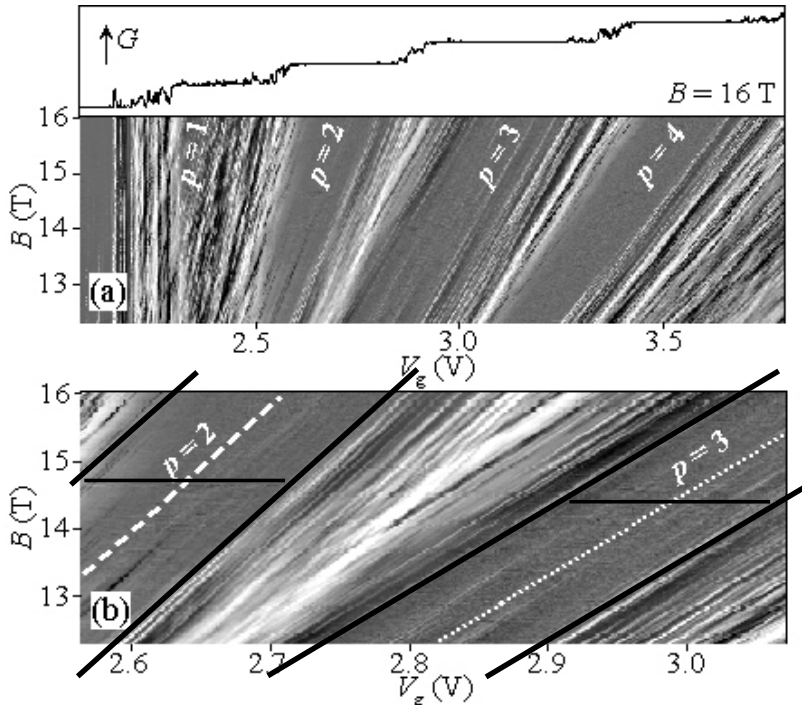

Figure 4. Greyscale plot of conductance with a smooth background substracted (lighter = smaller G, where G is the Hall conductance) taken from [13]. p denotes the filling factor. On (*b*), we have added oblique dark lines to indicate clearly the two stripes; their corresponding horizontal width are indicated by horizontal dark lines. It can be easily verified that both horizontal widths are equal.

prime integers q and p, there exist (necessarily) prime integers a and b such that

$$qb - pa = \pm 1. \tag{2.4}$$

Then, for any (q, p) vertex of the lattice with q odd, associate the set of points (a, b) satisfying this relation. It is easy to realize that these points are located on two parallel straight lines forming a stripe surrounding the (q, p) vertex as depicted in figure 3. We then obtain stripes for any odd denominator fraction p/q. Notice that the stripes can overlap, contrary to what happens for the even diagram†.

At this point, one remark is in order. In the odd diagram, the two parallel straight lines forming a stripe surrounding a given vertex (q_0, p_0) (together with the middle line passing through the origin) have a slope equal to p_0/q_0. This slope is, by construction, equal to the value of the filling factor ν.

2.3. Mapping the odd diagram to the V_g–B plane

We are now in a position to show that this latter diagram encodes interesting information concerning recent experimental work that has been reported in [13]. The corresponding result concerning the mesoscopic conductance in the quantum Hall regime in a silicon MOSFET is that the extrema for the conductance fluctuations spread on linear trajectories in the V_g–B plane parallel to constant (integer) filling factor. Recall that the quantum Hall fluctuations

† It is not difficult to see that the Haldane hierarchy is involved in the odd visibility diagram.

considered here are observed in the transition regions and are different from the two other types of fluctuations occurring at low B and low enough V_g, as mentioned in [13]. In [13], the relation (1.1) has been found to be verified to within a few percent accuracy. Furthermore, a stripe structure in the V_g–B plane has been observed, as shown in figure 4 (taken from figure 2 of [13]). Notice that our theoretical analysis strictly refers to the conductivity while the above experiment gives access to the conductance which is related to the former quantity by an overall geometrical factor, as is well known. But the properties of the stripe structures we consider in this paper do not refer to the actual value of the conductivity (or the conductance) so that figure 4 can be directly compared with our theoretical analysis. Now, observe that in the experiment [13] the gate voltage V_g varies linearly with the number of charge carriers N_c in the sample; furthermore, it is obvious that B varies linearly with the number of unit flux N_Φ.

In order to confront some of these experimental results with the present $\Gamma(2)$ framework, we have to exhibit a possible relation between the visibility diagram, the gate voltage and the applied magnetic field. This proceeds as follows. On the one hand, it is well known that the physical definition of the filling factor is given by

$$\nu = \frac{N_c}{N_\Phi}. \tag{2.5}$$

On the other hand, in the odd diagram, the filling factor is equal to the slope p/q of (the lines forming) the stripe surrounding the vertex (q, p), as already indicated in section 2.2. Bringing this together, this suggests identifying the (q, p) plane with the (N_Φ, N_c) plane, the latter being naturally related to the B–V_g plane. This gives rise to a mapping of the odd diagram to the B–V_g plane defined by†

$$q \mapsto B \qquad p \mapsto V_g. \tag{2.6}$$

The physical relevance of this mapping is supported by the following facts. First, observe that the action of the operator T^2 (2.3a) on any vertex (q, p) of the visibility diagram gives rise to a vertical shift

$$T^2 : (q, p) \to (q, p + 2q). \tag{2.7}$$

In the physical literature, T^2 has been identified with a Landau shift type operator, acting on the filling factor as $\nu \to \nu + 2$, which corresponds to an increase of the number of charge carriers. Next, observe that the action of the operator Σ (2.3b) on any vertex (q, p) is given by

$$\Sigma : (q, p) \to (q + 2p, p). \tag{2.8}$$

Physically, this operator is interpreted as the flux attachment operator, which then corresponds to an increase of the applied magnetic field B. This shows that the q and p axes on the odd diagram refer, respectively, to the B and N_c (or V_g) axes.

From the above defined mapping, it is now possible to perform a comparison between the stripe structure occurring in the V_g–B plane observed in [13] and the one stemming from the odd diagram. These structures are depicted respectively in figures 4 and 5. In figure 4, the stripe structure is indicated by grey areas (those indexed by filling factors $p = 1, 2, 3, 4$) which correspond clearly to Hall plateaux as can be easily seen on the upper onset of figure 4 where the conductance versus V_g is depicted. For the sake of clarity, we have delimited the stripes for $p = 2, 3$ by dark oblique lines in figure 4(b). Notice that, for the moment, we do not consider the fluctuations of the conductance, focusing only on the Hall plateaux. In order to make the comparison easier, we have only represented in figure 5 the stripes corresponding to integer filling factors $\nu = 1, 2, 3, 4$. We observe good qualitative agreement between both

† Up to dimension full factors.

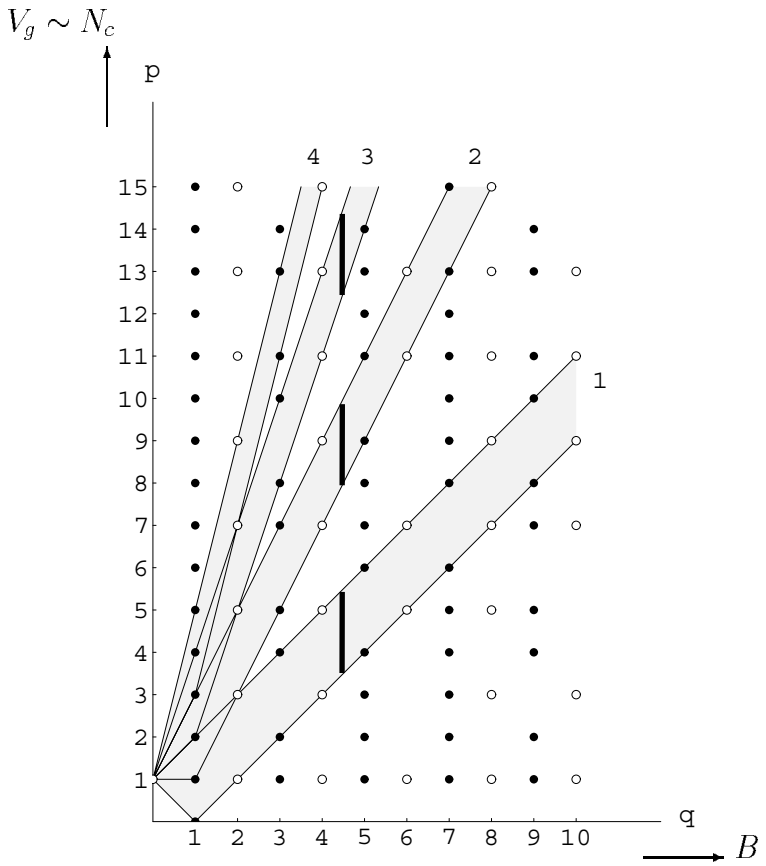

Figure 5. Selected stripes from the odd diagram corresponding to their experimental counterpart depicted in figure 4. Open dots represent fractions p/q with q even, full dots represent fractions with q odd. Notice that the horizontal (resp. vertical) axis is associated with B (resp. V_g) so that a direct comparison with figure 4 can be done after the axes have been permuted. Dark vertical lines indicate that the vertical widths for the stripes are equal.

structures. Each grey area in figure 4 corresponding to a given (integer) plateau appears to be bounded by two parallel straight lines (at least in the considered range for V_{g} and B). Taking into account the method for constructing the odd diagram, it is natural to identify each grey area associated with a given integer filling factor with the corresponding stripe in figure 5. Now, the experimentally verified equation (1.1) tells us that the slope of the two parallel lines delimiting each stripe in figure 4 depends only on the filling factor $\nu = n$ (integer) up to a dimension full factor while in figure 5 the slope for each corresponding stripe is exactly equal to the filling factor, as already mentioned. This dimension full factor could, of course, be related to those dimension full) factors necessarily appearing in the mapping (2.7).

Taking into account the above analysis, we now propose a physical interpretation of the stripes of the odd diagram: the (q, p) plane of the odd diagram is identified with the B–V_{g} plane of the experiment, any point inside a given stripe of the odd diagram being related to a Hall state whose Hall conductivity is equal to the slope of this stripe. Obviously, any real experiment can only reach a finite range of values for B and V_{g} so that only a finite number of stripes must be taken into account in the odd diagram for that experiment (very much as we

did in figure 5 in the case of the experiment performed in [13]). Within the present physical picture, even when the number of involved stripes is finite, it may happen that two stripes overlap partially. In this case, the above analysis does not apply for the overlapping areas. At the present time, we do not have a clear interpretation of the status of the points belonging to the overlapping areas.

It is possible to obtain from the odd diagram further information on the Hall conductance as a function of V_g (uppermost onset of figure 4) by adapting to the present situation, for which B is fixed while V_g (N_c) varies, the argument that we used in [10] to obtain a resistivity plot (Hall resistivity versus B), agreeing well with the experimental plot. This is straighforwardly achieved by simply assuming that the vertical width of any stripe in figure 5, defined by the intercept of any vertical line with that stripe, is proportional to the width of the corresponding plateau. The subsequent analysis is then very similar to the one that we described in [10]. We have found that the resulting conductivity–V_g plot agrees qualitatively with the one depicted in figure 4.

At this point, the analysis suggests that the proposed physical interpretation of the odd diagram is consistent with the experimental observations corresponding to the *integer* QHE. Proving that this diagram encodes some relevant properties of both integer and fractional QHE (giving therefore some global information on the phase diagrams) would require further comparison with experiments exploring the fractional quantum Hall regime (and/or for higher magnetic fields). In this regime, it is obvious from the very construction of the odd diagram that one (experimentally testable) prediction of the present scheme is the occurrence of branching tree-like structures [10] among the stripes in the V_g–B plane, similar to the one appearing in figure 3. We notice furthermore that the physical interpretation of the odd diagram is consistent with the Streda formula [18] given by

$$\sigma_{\mathrm{Hall}} = K \frac{\partial \rho}{\partial B} \tag{2.9}$$

where K is some constant, which has been proved under various hypotheses (see, e.g. [19] and references therein) and reduces to (1.1) when $\frac{\partial \rho}{\partial V_g} = C/e$. This can be very easily realized by observing that, within each stripe (which is associated with a plateau indexed by $p/q = \sigma_{\mathrm{Hall}} \cdot (\mathrm{constant})$), one has automatically $p/q = \sigma_{\mathrm{Hall}} \cdot (\mathrm{constant}) = \frac{\partial V_g}{\partial B}$ which reproduces (2.10) when $\frac{\partial \rho}{\partial V_g} = C/e$.

Let us now consider the quantum Hall fluctuations. Recall that these fluctuations are observed in the transition regions between plateaux which narrow as the temperature decreases while the fluctuations grow and sharpen. Fluctuations in the conductance have been studied for some time (see [21] and references therein), in particular those occurring in two-dimensional systems in high magnetic fields where the QHE dominates, but it appears in this latter case that relatively little is firmly known (compared with the low magnetic field case). As pointed out in, e.g. [21], neither of the two existing (microscopic) pictures used to explain the occurrence of fluctuations at high magnetic field is really applicable for experiments performed with Si MOSFET devices. Furthermore, one of the main conclusions of [13] pointed out that the experimental verification of (1.1) contradicts the predictions of non-interacting (single-particle) models and gave convincing arguments supporting the strong influence of charging effects in the behaviour of the quantum Hall fluctuations. Obviously, further experimental as well as theoretical studies are needed in order to build a (microscopic) model providing a realistic description of the observed quantum Hall fluctuations of the conductance. Such a construction is beyond the scope of this paper. Nevertheless, the fact that the physical interpretation of the odd visibility diagram presented in this paper is consistent with the experiments performed in [13] suggests that modular symmetries (or at least the present framework based on modular symmetries) may

well be an important ingredient for constructing and/or constraining a realistic model for the quantum Hall fluctuations of conductance. Such a model might possibly explain why the fluctuations of the conductance follow the pattern of the odd visibility diagram. Keeping in mind the above analysis, it seems plausible to conjecture that, for a given transition $\nu = n_1 \to \nu = n_2$, $n_{1,2} \in N$, which may be extended to $n_{1,2} \in Q$ if the present scheme applies to the fractional QHE, the directions of the two coexisting families of straight lines involving the extrema of the fluctuations (which are observed in [13] for the transitions $0 \to 1$, $1 \to 2$, $2 \to 3$, $3 \to 4$) are given by the directions defined by the corresponding stripes involved in that transition.

The relevance of the visibility diagrams in the description of the QHE motivates a deeper investigation of the mathematical properties underlying their structure. This is what we consider now.

3. More on visibility diagrams and discussion

First, we point out that the odd diagram is, in fact, the superposition of two 'more elementary' visibility diagrams. To see that, consider separately the odd and even *numerator* filling factors (with odd denominator) and apply the method for constructing the odd visibility diagram that has been described in section 2. Doing this, one obtains the two new diagrams represented in figures 6 and 7 corresponding, respectively, to odd and even *numerator* filling factors (hereafter called, respectively, the odd/odd and even/odd diagrams). Then, it can be easily realized that the superposition of these two latter diagrams gives rise to the odd visibility diagram. Note that the stripes appearing in these two diagrams do not overlap as is the case for the even diagram. Furthermore, observe that this latter diagram is related to the even/odd diagram through a symmetry around the $p = q$ axis which corresponds to the action of an operation belonging to the full modular group $\Gamma(1)$ but *not* to $\Gamma(2)$.

Let us study more closely the action of modular transformations pertaining to $\Gamma(1)$ on the even, even/odd and odd/odd diagrams. Some remarks are in order. On the one hand, it can be easily seen that the action of any $G \in \Gamma(1)$ preserves the arithmetic relation (2.4) ruling the whole construction of these diagrams. As a consequence, the action of $\Gamma(1)$ maps the stripe structure of each of the diagrams into another one or possibly a substructure. On the other hand, any $G \in \Gamma(2)$ maps each of these three diagrams into itself simply because $\Gamma(2)$ preserves the even or odd character of both numerator and denominator involved in the filling factor. In other words, the whole structure of each diagram remains invariant under $\Gamma(2)$. In fact, it appears that $\Gamma(2)$ is the largest subgroup of $\Gamma(1)$ leaving invariant each of the three diagrams. To see that, consider the action of the coset group $\Gamma(1)/\Gamma(2)$ on these diagrams. It is known in the mathematical literature [20] that this coset group involves six elements whose corresponding representatives in $\Gamma(1)$ can be chosen as

$$I = \begin{pmatrix} 1 & 0 \\ 0 & 1 \end{pmatrix} \tag{3.1a}$$

$$U = \begin{pmatrix} 1 & 1 \\ 0 & 1 \end{pmatrix} \tag{3.1b}$$

$$V = \begin{pmatrix} 0 & -1 \\ 1 & 0 \end{pmatrix} \tag{3.1c}$$

$$W = \begin{pmatrix} 1 & 0 \\ 1 & 1 \end{pmatrix} \tag{3.1d}$$

$$P = \begin{pmatrix} 0 & -1 \\ 1 & 1 \end{pmatrix} \tag{3.1e}$$

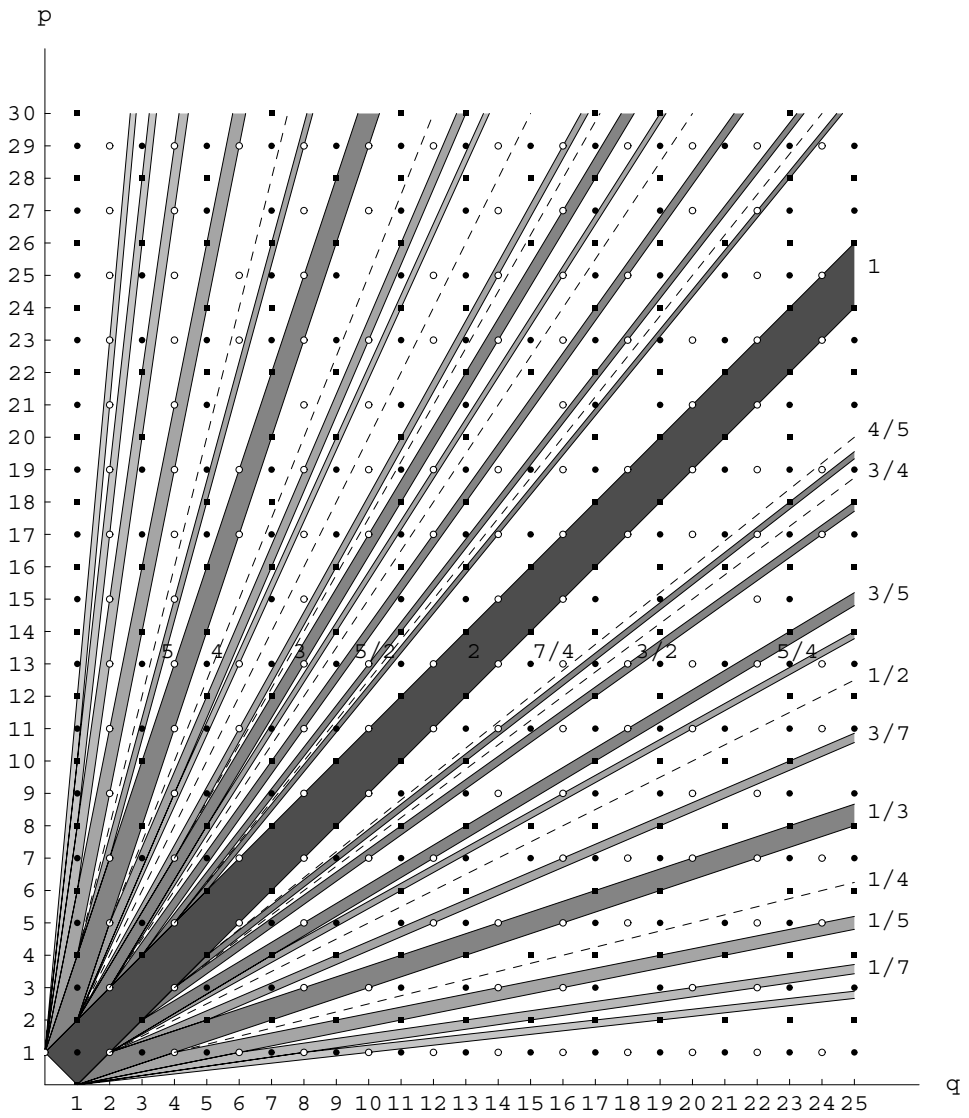

Figure 6. Odd/odd elementary diagram corresponding to filling factors with odd numerator and denominator. Open dots represent fractions p/q with q even, full dots represent fractions with q odd and p odd, and full squares represent fractions with q odd and p even.

$$P^2 = \begin{pmatrix} -1 & -1 \\ 1 & 0 \end{pmatrix} \tag{3.1f}$$

from which it can be verified that any of the six coset group elements maps a visibility diagram into a subdiagram included in another diagram. Finally, using (3.1) together with the definition of $\Gamma(2)$, it is easy to prove that the even and odd diagrams (depicted respectively in figures 1 and 3) are invariant under the action of another subgroup of $\Gamma(1)$ generated by U given by (3.1*b*) and $\Gamma(2)$. This subgroup is nothing but $\Gamma_0(2)$, which has been proposed [7] (see also the second of [6]) as another candidate for a discrete symmetry group underlying the physics of the QHE.

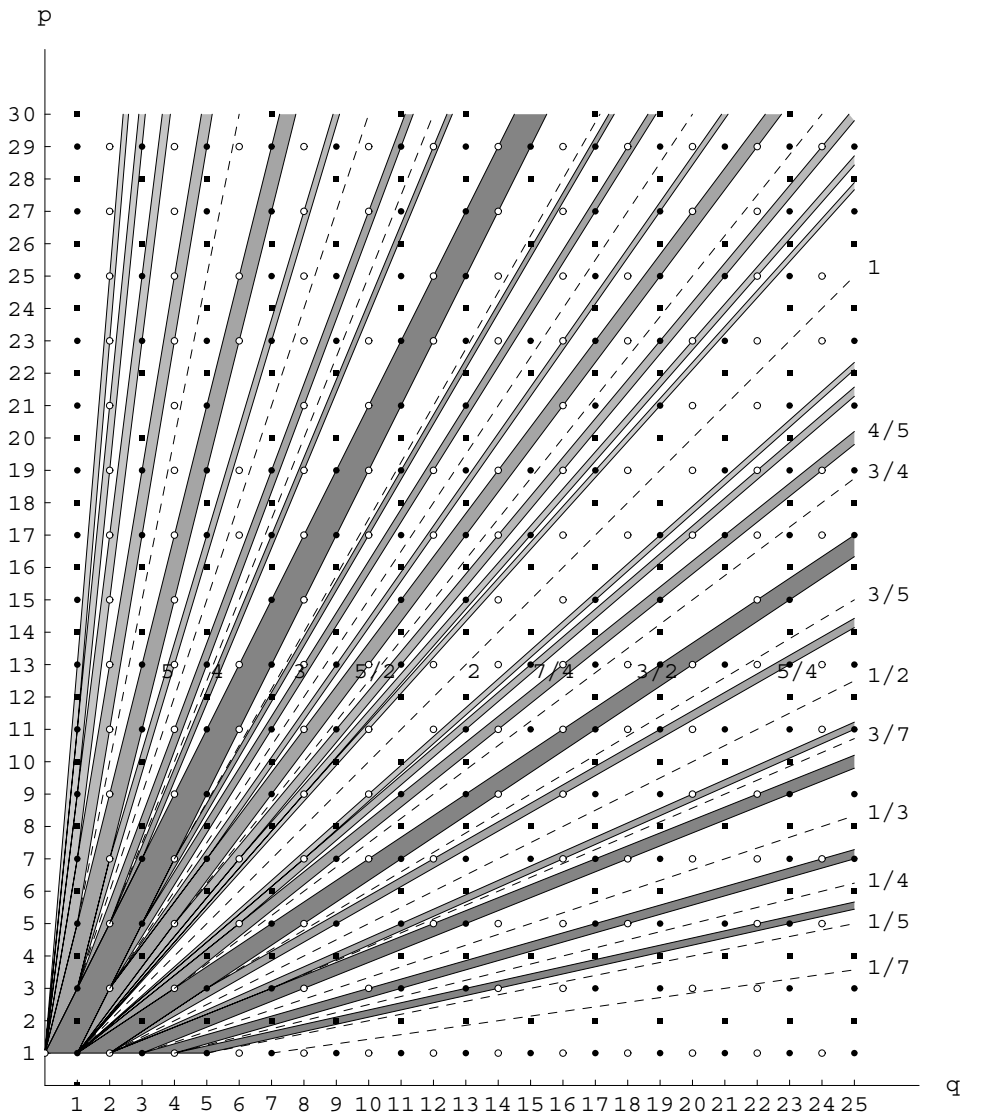

Figure 7. Even/odd elementary diagram corresponding to filling factors with even numerator and odd denominator. Open dots represent fractions p/q with q even, full dots represent fractions with q odd and p odd, and full squares represent fractions with q odd and p even. This diagram is related to figure 1 through the symmetry around the $p = q$ axis.

Note that the constraints from $\Gamma_0(2)$ on the renormalization group flow in a two-parameter scaling framework have been examined in [7]. The resulting flow diagram (phase diagram) has been shown to exhibit a specific feature. In fact, consistency with the present experimental observations requires the occurrence for the $0 \to 1$ transition† of a critical point at $\sigma_{xy} = \sigma_{xx} = 1/2$ which appears as a pole of the corresponding β function. This stems from the existence of a fixed point of $\Gamma_0(2)$ in its fundamental domain at $z_0 = (1+\mathrm{i})/2$ (recall that,

† Recall that, as usual, the whole flow diagram is obtained by applying successive $\Gamma_0(2)$ transformations to the $0 \to 1$ 'template' transition.

in this framework, one has $z = \sigma_{xy} + i\sigma_{xx}$ which parametrizes the conductivity plane). The situation is different in the $\Gamma(2)$ case, as shown recently in [11]: there is no critical point showing up as a pole (at finite distance in the conductivity plane) of the corresponding β function but consistency with the two-parameter scaling hypothesis seems to require the occurrence in each allowed transition of a temperature-independent point that might be identified with the crossing point appearing in the crossover of the observed transitions [11].

4. Conclusion

Let us summarize the results involved in this paper. We have analysed various properties of the visibility diagrams which are related to the modular symmetries. In particular, we have shown that the observed structures occurring in the (gate voltage–magnetic field) data, at least in the integer quantum Hall regime, may well be encoded in one visibility diagram, namely the odd one. We have also indicated an experimental way to test its possible relevance to the fractional QHE. Furthermore, we have conjectured that, for a given transition $\nu = n_1 \to \nu = n_2$, $n_{1,2} \in Q$, the directions of the two coexisting families of straight lines involving the extrema of the fluctuations (observed in [13] for the transitions $0 \to 1, 1 \to 2, 2 \to 3, 3 \to 4$) are given by the directions defined by the corresponding stripes of the odd diagram involved in that transition. The consistency of the experimental results reported in [13] with the present framework suggests that this latter (or some of its modular symmetry counterpart) may well encode features of the dynamics ruling the conductance fluctuations in the quantum Hall regime.

References

[1] R E Prange and S M Girvin (ed) 1990 *The Quantum Hall Effect* 2nd edn (New York: Springer)
See also Sorma S D and Pinczuk A (ed) 1997 *Perspectives in Quantum Hall Effect* (New York: Wiley)
[2] von Klitzing K, Dorda G and Pepper M 1980 *Phys. Rev. Lett.* **45** 494
[3] Tsui D C, Störmer H L and Gossard A C 1982 *Phys. Rev. Lett.* **48** 1559
[4] Laughlin R B 1983 *Phys. Rev. Lett.* **50** 1385
Haldane F D 1983 *Phys. Rev. Lett.* **51** 605
Halperin B I 1984 *Phys. Rev. Lett.* **52** 1583
[5] Lütken C A and Ross G G 1992 *Phys. Rev.* B **45** 11 837
Lütken C A and Ross G G 1993 *Phys. Rev.* B **48** 2500
[6] Lütken C A 1993 *Nucl. Phys.* B **396** 670
Burgess C P and Lütken C A 1999 *Phys. Lett.* B **451** 365
See also Fradkin E and Kivelson S 1996 *Nucl. Phys.* B **474** 543
[7] Dolan B P 1999 *J. Phys. A: Math. Gen.* **32** L243
Dolan B P 1999 *Nucl. Phys.* B **554** 487
[8] Dolan B P 2000 Duality in the quantum Hall effect—the role of the electron spin *Preprint* cond-mat/0002228
[9] Georgelin Y and Wallet J C 1997 *Phys. Lett.* A **224** 303
[10] Georgelin Y, Masson T and Wallet J C 1997 *J. Phys. A: Math. Gen.* **30** 5065
[11] Georgelin Y, Masson T and Wallet J C 2000 *J. Phys. A: Math. Gen.* **33** 39
[12] Kivelson S, Lee D H and Zhang S C 1992 *Phys. Rev.* B **46** 2223
[13] Cobden D H, Barnes C H and Ford C J B 1999 Quantum Hall fluctuations and evidence for charging in the quantum Hall effect *Preprint* cond-mat/9902154
[14] Kravchenko S V, Mason W and Furneaux J E 1995 *Phys. Rev. Lett.* **75** 910
[15] Kravchenko S V *et al* 1995 *Phys. Rev.* B **51** 7038
[16] Hilke M *et al* 1999 Experimental phase diagram of the integer quantized Hall effect *Preprint* cond-mat/9906212
[17] Sheng D N and Weng Z Y 1999 Phase diagram of the integer quantum Hall effect *Preprint* cond-mat/9906261
[18] Streda P 1982 *J. Phys. C: Solid State Phys.* **15** L717
Streda P 1982 *J. Phys. C: Solid State Phys.* **15** L1299
[19] Dana I, Avron Y and Zak J 1985 *J. Phys. C: Solid State Phys.* **18** L679 and references therein
[20] See in Mumford D 1983 *Tata Lectures on Theta Functions* vol 1–3 (Boston, MA: Birkhauser)
[21] See Cobden D H and Kogan E 1996 *Phys. Rev.* B **54** R17 316 and references therein